Manganese(II)-Dependent Extradiol-Cleaving Catechol Dioxygenase from *Arthrobacter globiformis* CM-2[†]

Adam K. Whiting,[‡] Yvonne R. Boldt,[§] Michael P. Hendrich,[||] Lawrence P. Wackett,[⊥] and Lawrence Que, Jr.*[,‡]

Departments of Chemistry and Microbiology, University of Minnesota, Minneapolis, Minnesota 55455, Department of Biochemistry and Institute for Advanced Studies in Biological Process Technology, University of Minnesota, St. Paul, Minnesota 55108, and Department of Chemistry, Carnegie Mellon University, Pittsburgh, Pennsylvania 15213

Received August 21, 1995; Revised Manuscript Received November 2, 1995[⊗]

ABSTRACT: A manganese-dependent 3,4-dihydroxyphenylacetate 2,3-dioxygenase from *Arthrobacter globiformis* strain CM-2 (MndD) cloned in *Escherichia coli* has been purified to homogeneity. Sedimentation equilibrium analysis indicates an α_4 homotetrameric holoenzyme structure ($4 \times 38\,861$ Da). Steady-state kinetic analysis of MndD with a variety of substrates and inhibitors yields very similar relative rates to the known Fe(II)- and Mn(II)-dependent 3,4-dihydroxyphenylacetate 2,3-dioxygenases from *Pseudomonas ovalis* and *Bacillus brevis*, respectively. Yet, unlike the Fe(II)-dependent enzyme, MndD retains almost all activity in the presence of H_2O_2 and CN^- and is inactivated by Fe(II). ICP emission analysis confirms the presence of 3.0 ± 0.2 g-atoms Mn (and only 0.7 ± 0.2 g-atoms Fe) per tetrameric holoenzyme molecule. Comparison of MndD samples with varying metal content, including an apo and partial-apo enzyme preparation, shows a strong positive correlation between specific activity and Mn content. EPR spectra of MndD as isolated exhibit a nearly isotropic $g = 2.0$ signal having 6-fold hyperfine splitting ($A = 95$ G) typical of octahedrally coordinated Mn(II) in a protein. Quantitation of the EPR spin yields 3.4 ± 0.3 g-atoms of Mn(II) per holoenzyme. When exposed anaerobically to its natural substrate, 3,4-dihydroxyphenylacetate (3,4-DHPA), the EPR spectrum undergoes a dramatic change characterized by the attenuation of the $g = 2$ signal and the appearance of new signals at $g = 1.2$, 2.9, 4.3, and 16. The $g = 4.3$ signal displays 6-fold hyperfine splitting ($A = 95$ G) that unambiguously assigns it to the Mn(II) center. The appearance of these new signals indicates a large increase in zero-field splitting suggestive of a change in ligand coordination to the Mn(II) center. Similarly perturbed signals are seen in the EPR spectra of MndD complexed with the comparably active substrate analog, D,L-3,4-dihydroxymandelate, or the tight-binding inhibitor, *p*-nitrocatechol, but not in the complexes with weaker binding substrates and inhibitors. The fact that only strong-binding substrates and inhibitors significantly perturb the Mn(II) EPR signal strongly suggests that the substrate coordinates to the Mn(II) center in the catalytic pathway.

The catechol dioxygenases catalyze the cleavage of dihydroxybenzene rings with the incorporation of molecular oxygen. Two families of catechol dioxygenases have been identified on the basis of the position of ring cleavage: intradiol, which cleaves the carbon−carbon bond between the two hydroxyls of the catechol; and extradiol, which cleaves the carbon-carbon bond adjacent to the enediol moiety. Although they share many substrates, the intra- and extradiol cleaving enzymes exhibit exclusivity in their products indicating the existence of two distinctly different catalytic mechanisms (Lipscomb & Orville, 1992; Lipscomb et al., 1982; Que, 1989). Whereas every intradiol dioxygenase has been found to contain Fe(III) as the active metal center, all but three extradiol dioxygenases have been found to contain Fe(II) (Lipscomb & Orville, 1992). The three exceptions include the recent report of a Mg(II)-dependent enzyme (Gibello et al., 1994) and two which depend on Mn(II) (Qi, 1991; Que et al., 1981). Hence, the elucidation of these two mechanisms appears to lie in understanding the structural and chemical features of the different metal centers. The greater spectroscopic accessibility of Fe(III) has led to the acquisition of a much larger body of work on the intradiol dioxygenases and a detailed mechanism has been proposed (Que, 1989; Lipscomb & Orville, 1992). A renewed focus on the extradiol cleavage mechanism has come about as the result of several recent advances including MCD[1] (Mabrouk et al., 1991) and EXAFS (Bertini et al., 1994; Shu et al., 1995) analyses of the catechol 2,3-dioxygenase from *Pseudomonas putida* mt-2 and its substrate complex, and the crystal structure of the Fe(II)-dependent 2,3-dihydroxybiphenyl 1,2-dioxygenase from *Pseudomonas* sp. strain LB400

[†] This work was supported by National Institutes of Health Grants GM 43315 (L.Q. and L.P.W.), GM 33162 (L.Q.), and GM 49970 (M.P.H.).

* Author to whom correspondence should be addressed.

[‡] Department of Chemistry, University of Minnesota, Minneapolis.

[§] Department of Microbiology, University of Minnesota, Minneapolis.

[||] Department of Chemistry, Carnegie Mellon University, Pittsburgh.

[⊥] Department of Biochemistry and Institute for Advanced Studies in Biological Process Technology, University of Minnesota, St. Paul.

[⊗] Abstract published in *Advance ACS Abstracts,* December 15, 1995.

[1] Abbreviations: MndD, Mn(II)-dependent 3,4-dihydroxyphenylacetate 2,3-dioxygenase; BphC, Fe(II)-dependent 2,3-dihydroxybiphenyl 1,2-dioxygenase; 3,4-DHPA, 3,4-dihydroxyphenylacetic acid; 5-CHMSA, 5-(carboxymethyl)-2-hydroxymuconic semialdehyde; P_i, phosphate; MOPS, 3-(*N*-morpholino)propanesulfonic acid; bis-tris, [bis(2-hydroxyethyl)imino]tris(hydroxymethyl)methane; CHES, 2-(*N*-cyclohexylamino)ethanesulfonic acid; tricine, *N*-tris(hydroxymethyl)methylglycine; EPR, electron paramagnetic resonance; ICP, inductively coupled plasma; MCD, magnetic circular dichroism; EXAFS, extended X-ray absorption fine-structure.

0006-2960/96/0435-160$12.00/0

(BphC) (Sugiyama et al., 1995; Han et al., 1995). Toward the goal of understanding the extradiol cleavage mechanism, the existence of the Mn(II)-dependent enzymes permits the possibility of direct EPR observation of changes at the active metal center during catalysis. Perhaps more intriguing, the existence of the Mn(II)-dependent enzymes has provoked two questions: (1) What, if any, functional/mechanistic differences exist between the Fe(II)- and Mn(II)-dependent enzymes? and (2) What structural features of the protein determine the preference of one metal over the other? These same questions have arisen in the context of the Fe- versus the Mn-dependent superoxide dismutases, and they remain largely unanswered even in light of well-resolved crystal structures of the two sites (Lah et al., 1995).

Unfortunately, the original *Bacillus brevis* strain with the first Mn(II)-dependent enzyme was lost and these questions remained dormant for several years until the discovery of the Mn(II)-dependent 3,4-DHPA 2,3-dioxygenases in *Arthrobacter* Mn-1 and *Arthrobacter globiformis* strain CM-2 (Olson et al., 1992; Qi, 1991). Recently the gene *mndD* which codes for the enzyme from strain CM-2 has been cloned and sequenced in *Escherichia coli*. (Boldt et al., 1995). Analysis of the *mndD* sequence shows it to be a member of the major Fe(II)-dependent extradiol dioxygenase enzyme family containing 14 of 18 conserved amino acid residues, six of which are potential metal ligands (Boldt et al., 1995). By homology to the sequence of BphC, whose structure has been solved crystallographically (Sugiyama et al., 1995; Han et al., 1995), three residues in the *mndD* sequence, H155, H214, and E267, have been proposed as the most likely metal coordinating ligands (Boldt et al., 1995).

In the work described here, the enzyme, MndD has been isolated and purified to homogeneity. The size, metal content, and functional characteristics of the purified enzyme have been determined, and it is concluded that MndD represents a new example of an extradiol-cleaving dioxygenase that is dependent on Mn(II) to activate dioxygen. EPR analysis of the anaerobic complexes of MndD with a variety of substrates and inhibitors suggests the formation of a directly coordinated Mn−substrate complex as the first intermediate in the catalytic mechanism.

MATERIALS AND METHODS

Sources of Materials. All substrates, inhibitors, and buffer salts were obtained from Aldrich Chemical and used without further purification. DNase I, lysozyme, and the protease inhibitors PMSF, benzamide, benzamidine, leupeptin, and antipain were obtained from Sigma. DEAE Sepharose Fast-Flow gel was obtained from Pharmacia.

Bacterial Growth Conditions. E. coli containing the MndD gene from *Arthrobacter globiformis* CM-2 was grown in LB media (20 g of tryptone/L, 10 g of yeast extract/L, 10 g of NaCl/L, pH 7.2) at 37.5 °C in a 24 L fermentor at the facilities of the Biological Process Technology Institute (University of Minnesota, St. Paul, MN). Initially, 100 mg of ampicillin/L was present followed by a supplemental addition of 1.5 g after 3 h. 150 μM $MnCl_2 \cdot 4H_2O$ was also added as its presence in previous smaller scale preparations was shown to increase the MndD specific activity of the crude extract. A total of 300 g of wet cell paste was obtained from the 24 L fermentation and stored frozen at −80 °C until used in purification.

Enzyme Purification. 100 g of *E. coli* wet cell paste was suspended in 250 mL of 50 mM KP_i buffer, pH 7.5, containing a protease inhibitor cocktail of PMSF (1 mM), benzamide (1 mM), benzamidine (1 mM), leupeptin (1 μg/mL), and antipain (1 μg/mL) as well as lysozyme (0.2 mg/mL) and DNase I (0.02 mg/mL). The suspension was incubated for 30 min at room temperature, then sonicated twice at 100 W for 3 min, and centrifuged at 15 000*g* for 30 min to yield 300 mL of cell-free crude extract. The crude extract was transferred to an Erlenmeyer flask into which an equivalent volume (300 mL) of cold acetone (−45 °C) was added drop-wise over a 1 h period with constant stirring. The resulting 50% acetone suspension was immediately centrifuged for 10 min at 27 000*g*, and −10 °C, yielding a large amount of precipitate and approximately 550 mL of a clear yellow supernatant. The supernatant was decanted, immediately diluted with an additional 50 mL of pH 8.0 buffer (50 mM KP_i, 0.1 M KCl, plus the inhibitor cocktail) to prevent any further acetone-induced precipitation, and then loaded at 3 mL/min onto a DEAE Sepharose Fast-Flow ion-exchange column (5 cm i.d. × 10 cm high) equilibrated with the pH 8.0 buffer. After being washed with 1200−1500 mL of the starting buffer, the column was eluted at 100 mL/h with a 0.1−0.5 M KCl gradient in 500 mL total volume. The MndD activity eluted in a large A_{280} peak at 0.33−0.35 M KCl. The most active fractions were pooled and concentrated to 45 mL using an Amicon PM30 membrane, and then twice rediluted and reconcentrated in pH 6.3 buffer (50 mM bis-tris plus the inhibitor cocktail). This final concentrate was applied to a Pharmacia Mono-Q 16/10 FPLC column equilibrated with the pH 6.3 buffer, and eluted at 2.0 mL/min with a 0.2−0.4 M KCl gradient in 160 mL total volume. The enzyme activity eluted in a single, slightly asymmetric A_{280} peak at 0.27 M KCl concentration. After the MonoQ column, the purity of the MndD was analyzed using polyacrylamide gel electrophoresis (Laemmli, 1970). The gel plates (16 × 16 cm) were prepared with a 4% stacking gel above a 12% separating gel and loaded with 10−15 μg of protein which had been treated by 5 min of boiling in a buffer solution containing 5% β-mercaptoethanol and 2% SDS. The Sigma SDS-7 set of low molecular mass proteins (bovine albumin, 66 kDa; egg albumin, 45 kDa; rabbit glyceraldehyde-3-phosphate dehydrogenase, 36 kDa; carbonic anhydrase, 29 kDa; trypsinogen, 24 kDa; trypsin inhibitor, 20.1 kDa; and α-lactalbumin, 14.2 kDa) was used as a standard. The gels were stained with Coomassie Blue R-250. Overloaded wells containing 40 μg of protein were also prepared and confirmed the homogeneity of the MndD preparation.

Amino Acid Analysis. Quantitative amino acid analysis of purified MndD was carried out by the Microchemical Facility of the Human Genetics Institute (University of Minnesota, Minneapolis, MN). The MndD sample solution (150.0 μL of 15−20 μg of purified enzyme in 0.1 M MOPS buffer, pH 7.6) was hydrolyzed under vacuum in 6 N HCl, 1.5% (v/v) phenol at 110 °C for 24 h and then analyzed in a Beckman System 6300 high-performance analyzer. The previously measured A_{280} of the purified MndD sample and the total micrograms of protein as determined by the amino acid analysis yielded an extinction coefficient at 280 nm of 2.36×10^5 M^{-1} cm^{-1} (or $A_{280}^{0.1\%} = 1.52$; 100 mM MOPS

buffer, pH 7.6, 23 °C) for the enzyme. The determined MndD amino acid composition was in good agreement with the composition on the basis of the *mndD* gene sequence (Boldt et al., 1995), as well as with the amino acid composition determined for the *Arthrobacter* Mn-1 enzyme (Qi, 1991).

Sedimentation Equilibrium Analysis. Sedimentation equilibrium analysis was carried out to determine the holoenzyme molecular weight of the purified MndD. A meniscus-depletion experiment was carried out on a Beckman model E analytical ultracentrifuge with a Rayleigh interferometric optical system. A 1 mL 0.38 mg/mL sample of MndD was dialyzed for 24 h at 3 °C against 1 L of 50 mM KP_i buffer, pH 8.0, to ensure elimination of any small molecule contaminants, and this sample was then run in a double-sector cell at 10 588 rpm, 6.1 °C, for 52 h. Photographic plates of the interference fringes obtained after 50 and 52 h of spinning confirmed that equilibrium had been attained. The fringe displacements with respect to radius were measured from the photographic plates using a Nikon model 6C comparator. The plot of radius-squared versus the natural logarithm of the fringe displacement was fitted by the method of least-squares, resulting in a slope of 1.218 with an $R^2 = 0.999$. The density of the buffer was determined to be 1.008 g/mL at 6.1 °C, and the specific volume, ν, was determined to be 0.726 mL/g on the basis of the known sequence and the specific volume of the amino acids [taken from Schachman (1957)]. With the above data, the molecular mass was determined to be 172 000 Da, which is slightly greater than the homotetramer mass calculated from the known subunit mass ($4 \times 38\,861 = 155\,444$ Da).

Assays of Enzyme Activity. Aliquots taken after the various steps of the purification protocol were assayed for MndD activity by spectrophotometrically monitoring the turnover of the substrate, 3,4-dihydroxyphenylacetic acid (3,4-DHPA) to the extradiol product, 5-carboxymethyl-2-hydroxymuconic semialdehyde (5-CHMSA) at 380 nm. Assays were carried out by adding 10 μL of 0.05−0.2 mg/mL protein solution to 990 μL of buffer (50 mM KP_i, pH 8.0) containing 0.75 mM 3,4-DHPA at 23 °C. The extinction coefficient of 5-CHMSA at 380 nm was previously determined in 50 mM Tris buffer, pH 7.5, 20 °C, to be 36 000 cm^{-1} M^{-1} (Kita, 1965). Using this literature value, the extinction coefficient of 5-CHMSA (produced by the complete turnover of 3,4-DHPA in the presence of a large excess of MndD) in 50 mM KP_i buffer, pH 8.0, 23 °C, was determined to be 42 700 M^{-1} cm^{-1}. A unit of enzyme activity was defined as the amount that oxidizes 1 μmol of 3,4-DHPA per minute. The specific activity of MndD for the various purification steps (as reported in the first four rows of Table 1) was defined as the number of units of MndD activity per milligram of protein as measured with the Bradford protein assay using a BSA calibration standard (Bradford, 1976). The lower set of numbers in the fourth row of Table 1 reports the protein concentration and specific activity determined spectrophotometrically using the extinction coefficient for purified MndD ($A_{280}^{0.1\%} = 1.52$).

Examination of the absorbance spectra of 5-CHMSA over the pH range 6.3−9.8 revealed a clear isosbestic point at 350 nm due to an equilibrium between species having absorbance bands at 325 nm (apparent only below pH 7.5) and 380 nm. The extinction coefficient of 5-CHMSA at the 350 nm isosbestic point was determined to be 13 900 M^{-1} cm^{-1}. The pH dependence of MndD activity was determined by assaying activity at this pH-independent isosbestic wavelength. Assays were carried out in the usual manner described above but in a buffer appropriate for the pH (pH 6.3, 50 mM bis-tris; pH 7.0, 7.5, 7.75, and 8.0, 50 mM KP_i; pH 8.25, 8.5, and 8.85, 100 mM tricine; pH 9.0, 9.4, and 9.8, 100 mM CHES). Above pH 8.0 it was necessary to correct the observed rates for the base-catalyzed autooxidation of the substrate which produces significant absorption increase with time at 350 nm. A plot of the logarithm of the observed rate constants versus pH shows a clear plateau of maximum activity between pH 7.0 and 8.2.

The assays of relative activity as reported in Table 2 were carried out by adding 10 μL of a 5.3 or 0.53 μM MndD solution to 990 μL of a 1.25 mM solution of the given substrate in 50 mM KP_i buffer, pH 7.5. For the very slow substrates, 3,4-dihydroxybenzoic acid and 3-hydroxytyramine, the concentration of the 10 μL enzyme aliquot used was 130 and 270 μM, respectively. The rate of appearance of the extradiol product was monitored at the given λ_{max} [taken from Ono-Kamimoto (1973)]; the relative activity

Table 1: Purification of MndD

purification step	total activity[a] (units)	total protein[b] (mg)	specific activity[b] (units/mg)	purification factor	% yield activity
crude extract	2410	10 500	0.23	1	100
acetone extraction	1860	850	2.2	9.6	77
DEAE IEC	1600	480	3.3	14	66
MonoQ FPLC	1365	230	5.9	26	57
		150[c]	9.1[c]		

[a] A unit of enzyme activity was defined as the amount that oxidizes one micromole of 3,4-DHPA to 5-CHMSA per minute in 50 mM KP_i buffer, pH 8.0, 23 °C ($\epsilon_{380} = 42\,700$ M^{-1} cm^{-1}). [b] Protein concentration determined using Bradford assay and BSA standard. [c] Protein concentration determined using MndD extinction coefficient ($A_{280}^{0.1\%} = 1.52$).

Table 2: Steady-State Kinetic Parameters of MndD Catalysis and Inhibition

substrate/inhibitor	λ_{max} product[a] (nm)	relative activity[b]	k_{cat}[c] (min^{-1})	K_m[c] (μM)	K_i[d] (μM)
catechol−4-CH_2COO^-	380	100	1400	7	
catechol−4-$CHOHCOO^-$	375	54	1100	260	
catechol−4-$CH_2CH_2COO^-$	380	5.8	180	800	
catechol−4-CH_3	382	3.3			900
catechol	380	0.36			
catechol−4-COO^-	355	0.18			21 000
catechol−4-$CH_2CH_2NH_2$	413	0.0003			
catechol−4-NO_2					33
p-hydroxyphenylacetate					7000
m-hydroxyphenylacetate					500

[a] Taken from Ono-Kamimoto (1973). [b] Relative activities were measured by adding 10 μL of a 5.3 or 0.53 μM MndD solution to 990 μL of a 1.25 mM substrate solution (50 mM KP_i buffer, pH 7.5, 23.0 °C). The appearance of the extradiol product was monitored at the given λ_{max}. For the very slow substrates, 3,4-dihydroxybenzoate and 3-hydroxytyramine, the concentration of the MndD solution was 130 and 270 μM, respectively. [c] Assays were carried out by adding 10 μL of 0.20−0.50 μM MndD to each of six cuvettes containing 3,4-DHPA (ranging from 7.5 to 375 μM) and monitoring product appearance at 380 nm (50mM KP_i buffer, pH 8.0, 23 °C). The parameters k_{cat} and K_m were calculated by nonlinear regression analysis of the initial rates versus substrate concentrations. [d] Inhibition assays were carried out as described above but with the inclusion of the inhibitor in the assay solution before the final addition of enzyme. At least three different inhibitor concentrations were used, and the K_i values were extrapolated from a plot of apparent K_m versus inhibitor concentration.

Table 3: Inactivation of MndD

reagent	% activity remaining after incubation time at 3 °C[a] 15 min	3 h
1 mM H_2O_2	106	89
10 mM H_2O_2	98	60
1 mM NaN_3	105	97
1 mM 8-OH-quinoline	106	95
9 mM Na_2SO_4	98	98
4.8 mM NaCN	101	118
200 mM NaF	49	33
5 mM ascorbate	97	97
0.5 mM $MnSO_4$	103	107
4.8 mM $MnSO_4$	99	102
0.5 mM $Fe(NH_4)_2(SO_4)_2$	76	77
2.3 mM $Fe(NH_4)_2(SO_4)_2$	67	50
5 mM $K_3Fe(CN)_6$	95	90
5 mM $MgCl_2$	92	88
5 mM $ZnCl_2$	76	48

[a] 0.5 μM enzyme was incubated with the given concentration of reagent at 3 °C (0.1 M MOPS buffer, pH 7.5) for the given time, a 10 μL aliquot of this solution was added to 900 μL of 750 μM 3,4-DHPA (50 mM KP_i buffer, pH 8.0, 23.0 °C), and the appearance of product was monitored at 380 nm.

represents the observed rate divided by the rate measured with 3,4-DHPA, so these values should be considered estimates as no difference in the extinction coefficients of the various products was assumed.

Determination of the steady-state kinetic parameters, k_{cat}, K_m, and K_i, as reported in Table 2, was carried out by adding a 10 μL aliquot of MndD solution (0.20−0.50 μM) to each of six disposable cuvettes containing 3,4-DHPA (from 7.5 to 375 μM) and monitoring the appearance of product at 380 nm (50 mM KP_i, pH 8.0, 23 °C). The parameters k_{cat} and K_m were obtained from nonlinear regression analysis (Marquardt, 1963) of the initial rates versus substrate concentration using the Beckman DU-640 Enzyme Mechanism software. The concentration of MndD used for the calculation of k_{cat} was obtained spectrophotometrically using the holoenzyme extinction coefficient at 280 nm. K_i values for the various inhibitors were obtained under all of the same conditions described above with inhibitor present in the assay solution before the final addition of enzyme. At least three different inhibitor concentrations were used, and the K_i values for competitive inhibition were extrapolated from the *x*-intercept of the plot of the apparent K_m versus inhibitor concentration.

Determination of MndD Stoichiometry. In order to determine the catalytic stoichiometry, several assays were carried out in which 0.144 μmol of 3,4-DHPA was added to a 1.4 mL of a 0.040 μM MndD solution and total dioxygen uptake was measured with a YSI oxygen electrode (50 mM KP_i buffer, pH 8.0, 25 °C). Upon completion of dioxygen uptake (after approximately 10 min) the 5-CHMSA product was quantified spectrophotometrically (ϵ_{380} = 42 700 M^{-1} cm^{-1}). The stoichiometry of MndD catalysis was found to be 1.02−1.09 mol of dioxygen consumed for each mol of 5-CHMSA produced.

Assay of MndD Inactivation. Inactivation of MndD by the various metal ions and redox active reagents, as reported in Table 3, was measured by preincubating 0.5 μM MndD with the given concentration of reagent at 3 °C (0.1 M MOPS buffer, pH 7.5) for the given time and then adding a 10 μL aliquot to 990 μL of 750 μM 3,4-DHPA (50 mM KP_i, pH 8.0, 23 °C) and monitoring the appearance of product at 380 nm. Inactivation was measured as the percent activity remaining relative to a control assay of untreated MndD carried out simultaneously.

ICP Analysis. Samples for inductively coupled plasma (ICP) emission analysis were prepared using acid-washed glassware, Millipore-purified water, and TracePure grade HCl (Aldrich Chemicals). A 150.0 μL amount of 40−50 mg of purified enzyme/mL in pH 8.0, 50 mM KP_i buffer, was added to 2.35 mL of 20% HCl in a test tube which was then triply sealed with Dura-Seal film. A blank was made similarly using 150.0 μL of buffer instead of enzyme. The sealed tubes were then placed in a 90 °C water bath for 24−36 h, at which point all precipitated protein was fully hydrolyzed and the resulting solutions were transparent. The samples were then diluted to 10% HCl by the addition of water to a total volume of 5.00 mL and submitted for ICP analysis to the Research Analytical Laboratory (Department of Soil Science, University of Minnesota, St. Paul). The observed metal concentrations in the samples ranged from 0.30 to 1.5 ppm, with the blank concentrations less than 0.010 and 0.029 ppm for Mn and Fe, respectively. The blank Mn and Fe concentrations were subtracted before the metal content of the samples was calculated. The enzyme concentrations were determined from the A_{280} of the original stock enzyme solutions used before hydrolysis.

Apo-Enzyme Preparation. Apo-MndD was prepared by dialyzing 500 μL of 20 mg of MndD/mL for 48 h at 3 °C in 1 L of 0.1 M MOPS buffer, pH 7.0, containing 250 mM imidazole and 25 mM 8-hydroxyquinolinesulfonate followed by dialysis for 24 h in 1 L of 0.1 M MOPS buffer, pH 7.5, alone to remove excess imidazole and 8-hydroxyquinolinesulfonate. The imidazole is believed to act as a chaotropic agent that "loosens" the native folded protein structure such that the chelator can access the metal site. A control MndD sample was dialyzed over the same time period without imidazole or 8-hydroxyquinoline present. Assay of the specific activity of the apo-MndD sample showed it to be less than 0.5% of that of the dialyzed control sample (which retained full specific activity). The partial-apo MndD sample was prepared by dialysis for 15 h in 1 L of 0.1 M MOPS buffer, pH 6.8, containing only 50 mM imidazole and 5 mM 8-hydroxyquinolinesulfonate, followed by dialysis for 24 h in 0.1 M MOPS buffer, pH 6.8. Assay of the partial apo-MndD showed it to have 40% of the specific activity of the undialyzed control sample.

EPR Sample Preparation and Spectroscopic Methods. EPR samples were 0.25−0.30 mM in holoenzyme concentration (0.75−0.90 mM Mn), in 50 mM KP_i buffer, pH 8.0. Samples of 300 μL were inserted in 3.0 mm i.d. quartz tubes and frozen by slow immersion in liquid nitrogen. Anaerobic samples were prepared by repeated cycling under vacuum and argon of 250 μL of enzyme solution in the EPR tube followed by addition using a gas-tight syringe of 50 μL of concentrated substrate/inhibitor solution that had been degassed under argon.

EPR spectra were recorded at X-band (9.23 GHz) using a Varian E-109 spectrometer equipped with an Oxford Instruments ESR-10 liquid helium cryostat. Spectra were acquired at 2.5 K as a single 4 min scan from 0 to 8000 G using 0.020 mW power, 10 G modulation amplitude, and 100 kHz modulation frequency. A check of the g = 2.0 signal intensity to microwave power ratio confirmed that the signal

was not saturated at 2.5 K and 0.020 mW. Spin quantitation was performed by double integration of the first derivative of the absorption spectrum between 0 and 8000 G (Palmer, 1967). The spin standard used was an aqueous solution of either 0.559 or 1.21 mM $MnSO_4 \cdot H_2O$ whose spin concentration had been confirmed by comparision to a known CuEDTA spin standard. The standard spectrum was obtained on the same day, at the same temperature, and with the same instrumental parameters as the enzyme samples. The exact cross-sectional area of each sample tube used for spin quantitation was determined by measuring the height of a known volume in the tube. Spin quantitation of MndD spectra obtained at 2.5 and 20 K (both 0.020 mW at 9.23 GHz) on the same day showed only a 5%−7% variance in Mn(II) content.

RESULTS

Purification of MndD. The results of the purification of MndD from 100 g of wet cell paste are summarized in Table 1. The 50% acetone extraction step was especially effective, showing nearly a 10-fold increase in purity with only a 23% loss of total MndD activity. The use of only 30% acetone resulted in a substantially greater retention of activity (95%) but with a concomitant loss of purity. Furthermore, the protein contaminants that were not eliminated by a 30% acetone extraction were difficult to eliminate in the subsequent chromatographic steps; hence the gains in total activity were offset by lower final specific activity. The MndD activity eluted from the DEAE anion-exchange column near 0.33 M KCl, which was coincident with a symmetric A_{280} peak, but the active fractions eluted from the final FPLC MonoQ column in a slightly asymmetric band with a sharp front edge at 0.27 M KCl and a shoulder out to 0.32 M KCl. The enzyme was judged pure on the basis of SDS−PAGE which showed a single band (M_r = 40 kDa). Initial purifications also showed a significant band at 37 kDa which was presumed to be a proteolytic fragment and was eliminated from later purifications by the inclusion of a cocktail of protease inhibitors in the purification buffers.

Using the natural substrate, 3,4-DHPA, the catalytic stoichiometry of the purified MndD was confirmed to be one mole of dioxygen consumed per mole of extradiol cleavage product, 5-CHMSA, produced. Assays carried out over a range of pH from 6.3 to 9.3 revealed that maximal enzyme activity occurs between pH 7.2 and 8.2. The specific activity of the purified MndD varied from 5.3 to 6.3 units/mg in different preparations using the Bradford assay (with BSA standard) to measure protein concentration. However a significantly higher specific activity of 9.1 units/mg was determined using the MndD extinction coefficient at 280 nm ($A_{280}^{0.1\%}$ = 1.52; 50 mM KP_i buffer, pH 8.0, 23 °C). To date, seven separate purifications of MndD have been carried out, yielding specific activities from 7.4 to 9.1 units/mg for the final purified enzyme.

Steady-State Kinetics. Steady-state kinetic parameters that characterize the catalytic function of MndD with a variety of substrates and inhibitors are presented in Table 2. The column listing relative activities is a coarse measurement of substrate preference that can be compared to similar measurements made on the Mn- and Fe-dependent enzymes from *B. brevis* (Que et al., 1981) and *P. ovalis* (Ono-Kamimoto, 1973). The relative activities of the various substrates with MndD are generally the same as those observed for the *B. brevis* and *P. ovalis* enzymes indicating a similar preference for substrates with a carboxylate side chain. A Michaelis−Menten analysis was also carried out with a number of the substrates in order to determine values for k_{cat} and K_m. The K_m of MndD with the natural substrate, 3,4-DHPA, is 7 μM, only slightly lower than that of the *B. brevis* enzyme (K_m = 14 μM; Que et al., 1981). The k_{cat} of the MndD holoenzyme with 3,4-DHPA is 1400 min^{-1}, which corresponds to a specific activity of 9 units/mg which is in good agreement with that determined for the *B. brevis* enzyme. D,L-3,4-Dihydroxymandelate, which features an additional hydroxyl group on the side chain, has a 35-fold higher K_m of 260 μM but a nearly identical k_{cat}. K_m increases even further to 800 μM, and k_{cat} drops off significantly for (3,4-dihydroxyphenyl)propionate, which features an additional methylene group between the carboxylate and the catechol ring. On the other hand, shortening of the side chain by a methylene group, as in 3,4-dihydroxybenzoate, results in even lower relative activity and weaker binding, as demonstrated by a very high competitive K_i of 21 000 μM. Although 4-methylcatechol turns over almost 200-fold faster than 3,4-dihydroxybenzoate, attempts to measure its K_m were hindered by its ability to inhibit MndD at concentrations above 6 mM. It was possible to measure a competitive K_i of 900 μM for 4-methylcatechol. K_i values were also measured for the other substrate analogs, and in every case inhibition was found to be competitive. The very low K_i of *p*-nitrocatechol (33 μM) relative to the sterically very similar 3,4-dihydroxybenzoate and 4-methylcatechol was surprising as it had not been observed previously with any 3,4-DHPA 2,3-dioxygenase. Comparison of the K_i's of *m*- and *p*-hydroxyphenylacetate shows that 14-fold stronger inhibition occurs with the *meta*-substituted inhibitor, a result that also was observed for the *B. brevis* enzyme (Que et al., 1981). This observation supports the assertion that, in addition to the carboxylate, interactions of the substrate hydroxyls with the enzyme strongly determine substrate binding.

Inactivation of MndD. Table 3 shows the results of assays of MndD activity in the presence of various reagents which commonly alter metalloenzyme activity. H_2O_2, CN^-, and $K_3Fe(CN)_6$ all rapidly inactivate the Fe(II)-dependent extradiol dioxygenases (Kita, 1965) while having little effect on the Mn-dependent dioxygenases from *B. brevis* (Que et al., 1981) and *Arthrobacter* Mn-1 (Qi, 1991). The lack of MndD inactivation by 10 mM H_2O_2 and 5 mM CN^- supports the conclusion that Mn(II) and not Fe(II) is the catalytically essential cofactor. Because of its resistance to peroxide, MndD was examined for catalase activity but none was detected. However, there is significant loss (>40%) of MndD activity after long-term (over 3 h) exposure to 10 mM H_2O_2, which, unlike the Fe(II)-dependent enzyme from *P. ovalis*, cannot be restored by the addition of 1 mM $FeSO_4$ (Kita, 1965). In fact the presence of 0.5 mM $Fe(NH_4)_2(SO_4)_2$ (or $FeSO_4$) results in an immediate 25% decrease of MndD activity. Among other divalent cations, $MnSO_4$ and $MgCl_2$ have little effect but $ZnCl_2$ acts similarly to $Fe(NH_4)_2(SO_4)_2$, inactivating MndD by 24% after only 15 min. Like CN^- the anions N_3^-, SO_4^{2-}, and F^- have little or no effect on MndD activity, except at 200 mM where F^- decreases activity by 50% possibly due to its ability to bind to Mn(II).

Apo-MndD. In order to better characterize the correlation between metal content and MndD specific activity, a method

Table 4: Metal Content and Specific Activity of MndD

enzyme preparation	specific activity[c] (units/mg)	EPR spin quantitation[a] g-atoms of Mn per holoenzyme	ICP emission analysis[b] g-atoms of Mn per holoenzyme	ICP emission analysis[b] g-atoms of Fe per holoenzyme
1	7.4	3.1	3.1	1.0
2	9.1	3.3	3.1	0.6
3	8.6	2.7	3.3	0.5
4	7.4	3.1	2.8	0.6
5	8.8	3.6	2.8	0.7
6	8.4	3.4	3.0	0.6
partial-apo, 4	3.0	1.5	1.2	0.4
apo, 2	0.0084	<0.04	0.02	0.2

[a] Specific activities calculated from k_{cat} values measured as described in Table 2. [b] Spectra were recorded at 2.0−2.5 K as a single 4 min scan from 0 to 8000 G using 0.020 mW at 9.23 GHz on a Varian E-109 spectrometer equipped with an Oxford Instruments ESR-10 liquid helium cryostat. Spin quantitation was performed by double integration of the first-derivative spectrum between 0 and 8000 G. The spin standard was an aqueous solution of $MnSO_4 \cdot H_2O$ whose spectrum was obtained on the same day, at the same temperature, and with the same instrumental parameters as the enzyme samples. [c] Samples for ICP emission analysis were prepared by adding 150.0−200.0 μL of a 40−50 mg/mL purified enzyme solution to 2.50 mL of 20% TracePure HCl and hydrolyzing for 24 h at 90 °C. The hydrolyzed samples were diluted to a final volume of 5.00 mL (10% HCl concentration) and submitted for analysis to the Research Analytical Laboratory (Department of Soil Science, University of Minnesota, St. Paul, MN). The observed Mn concentrations in the samples ranged from 0.30 to 1.5 ppm, with blank concentrations less than 0.010 and 0.029 ppm for Mn and Fe, respectively.

of preparing an apo-enzyme was developed. While the metal-chelating reagent 8-hydroxyquinolinesulfonate at 1 mM concentration does not cause any decrease in MndD activity over a 3 h period, dialysis for 48 h at 3 °C in a 0.1 M MOPS buffer, pH 7.0, also containing 250 mM imidazole and 25 mM 8-hydroxyquinolinesulfonate results in MndD that has only 0.5% of the specific activity relative to MndD as isolated. While incubation of this apo-MndD for up to 6 h at 3 °C in the presence of 5 mM $MnSO_4$ results in no increase in activity, dialysis for 4 days in a 0.1 M MOPS buffer, pH 7.0, containing 250 mM imidazole and 25 mM $MnSO_4$ results in the recovery of 10% of the as isolated specific activity. A partial apo-MndD sample with 40% specific activity can be prepared by dialyzing against a slightly weaker chelating buffer (0.1 M MOPS, pH 6.8, 50 mM imidazole, 5 mM 8-hydroxyquinolinesulfonate) for 15 h.

Quantitation of MndD Metal Content. Table 4 shows the results of metal content analysis using ICP emission analysis and EPR spin quantitation of six different MndD preparations and the two apo-enzyme preparations. The values for specific activity are derived from values for k_{cat} determined by initial rate analysis as described above. The K_m values for the various preparations did not differ significantly. The ICP analysis of MndD as isolated yields an average Mn content of 3.0 ± 0.2 g-atoms per homotetramer and a Fe content of 0.7 ± 0.2 g-atoms per homotetramer. The partial-apo and apo-MndD preparations have Mn contents 60% and 99% lower, respectively, than the enzyme as isolated, which correlate well with their respective losses of 64% and 99% in specific activity. In contrast, the Fe contents of the partial-apo and apo preparations drop off only 43% and 66%, respectively. Although there is some variance among the specific activities of the six different MndD preparations, they show a strong positive correlation with Mn content when considered together with the apo and partial-apo preparations. The Fe contents, on the other hand, are scattered considerably and show little correlation with specific activity.

The Mn(II) content of MndD can also be determined by spin quantitation of its characteristic EPR signal (see next section). The values obtained are in agreement with the ICP analysis (Table 4), which suggests that Mn(III) is not present in any significant amount. Furthermore, ICP analysis of the buffer used to prepare the MndD samples shows only a trace (<0.05 μM) amount of free Mn present. Dialysis of a 241 μM MndD sample in this same buffer for 4 days results in no significant change in Mn or Fe content, demonstrating that loosely bound metal ions do not contribute to the ICP-determined metal content. The large variance in the EPR spin quantitation values most likely is due to the relative imprecision of this technique, where 5% error is possible only in the best circumstances (Palmer, 1967). Spin quantitations using spectra obtained on different days of the same sample were found to vary as much as 20%, while those obtained on the same day varied up to 7%. By contrast, the same MndD preparation hydrolyzed and analyzed by ICP on two separate occasions yielded only a 6% change in Mn and Fe content.

The Mn-dependent enzymes from *B. brevis* (Que et al., 1981) and *Arthrobacter* Mn-1 (Qi, 1991) were both found to contain 1.9−2.0 g-atoms of Mn per holoenzyme, with Fe ranging from 0.1 to 2.0 mol per holoenzyme. It should be noted, though, that these earlier measurements were carried out using the Lowry (1951) and Bradford (1976) methods to measure protein concentration, and, as mentioned previously, the Bradford method yields erroneous protein concentrations for MndD that are 50% higher than the extinction coefficient determined values. Consequently the Mn content determined using the Bradford concentration is 33% lower. Taking this difference into account, the previously determined values of 2 g-atoms of Mn per holoenzyme for the enzymes from *B. brevis* and *Arthrobacter* Mn-1 would most likely be corrected to the presently determined value of 3 g-atoms per holoenzyme.

Analysis of EPR Spectra. High-spin Mn(II) exists in an ^6S electronic state having zero orbital angular momentum and six degenerate spin states. The presence of a ligand field of less than cubic symmetry partially lifts the 6-fold degeneracy and creates zero-field splitting (ZFS) among the three Kramers doublets ($M_s = \pm 1/2, \pm 3/2, \pm 5/2$). In a magnetic field, the remaining degeneracies are lifted and five allowed ($\Delta M_s = \pm 1$) transitions can be observed in an EPR spectrum. Further complexity (and richness) of the system is introduced by the nuclear spin of ^{55}Mn, $I = 5/2$, which couples with the electron spin to create a 6-fold hyperfine splitting pattern and a total of 30 possible allowed ($\Delta M_s = \pm 1$, $\Delta M_I = 0$) transitions in the spectrum. Although this fine and hyperfine structure creates a distinct signature for Mn(II) EPR signals, it is often not fully resolved in the highly anisotropic outer fine-structure transitions ($\pm 5/2 \rightarrow \pm 3/2$, $\pm 3/2 \rightarrow \pm 1/2$) when Mn(II) is bound to a protein. Fortunately, the central fine-structure transition ($+1/2 \rightarrow -1/2$) is nearly isotropic and typically gives rise to an intense signal at $g = 2$ with resolved 6-fold hyperfine splitting. The magnetic spin levels of Mn(II) can be described by the spin hamiltonian (Abragam & Bleaney, 1970)

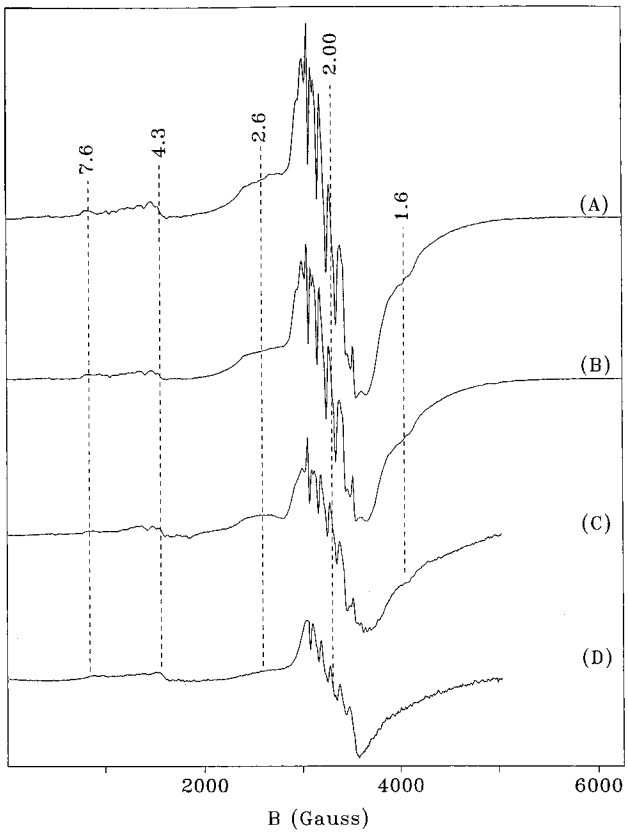

FIGURE 1: EPR spectra of (A) 0.260 mM purified MndD as isolated; (B) 0.260 mM MndD + 15.5 mM 4-methylcatechol, anaerobic; (C) 0.163 mM MndD + 80 mM *p*-hydroxyphenylacetatic acid; and (D) 0.174 mM MndD + 12.5 mM *m*-hydroxyphenylacetatic acid. Temperature, 2.5 K; power, 0.02 mW at 9.23 GHz; modulation amplitude, 10 G. All spectra are normalized to correct for differences in enzyme concentration and instrumental gain.

$$\mathbf{H} = g\beta\mathbf{B}\cdot\mathbf{S} + D(\mathbf{S}_z^2 - 35/12) + E(\mathbf{S}_x^2 - \mathbf{S}_y^2) + A\mathbf{I}\cdot\mathbf{S}$$

where D and E quantify the distortion of the ligand field from cubic and axial symmetry, respectively. Although the ZFS parameters D and E give ambiguous information regarding the coordination of the metal, the relative magnitudes of these parameters do reflect the degree of perturbation of inner-sphere metal−ligand coordination strength and geometry. Significant changes in the hyperfine coupling constant, A, also indicate changes in the covalency of the metal−ligand bonds.

The X-band (9.23 GHz) EPR spectrum of MndD at 2.5 K is shown in Figure 1A. The spectrum features a strong signal centered at $g = 2.00$ with well-resolved 6-fold hyperfine splitting which is characteristic of the central fine-structure transition ($+^1/_2 \rightarrow -^1/_2$). There are also two weaker shoulder-shaped signals at $g = 2.6$ and $g = 1.6$. These features are absent from the spectrum of apo-MndD, supporting their assignment to the catalytically essential Mn(II).

The expanded-scale spectrum of Figure 2A shows the hyperfine structure of the $g = 2.0$ signal of MndD to be more complicated than the typical six-line derivative signal observed for Mn(II). The five lowest-field hyperfine transitions each consist of a three-peak pattern. This additional structure is commonly observed in protein-bound Mn(II) and is attributed to forbidden transitions ($\Delta M_s = \pm 1$, $\Delta M_I = \pm 1$). The hyperfine coupling constant, A, measured directly from the spacing of the most intense derivative troughs is

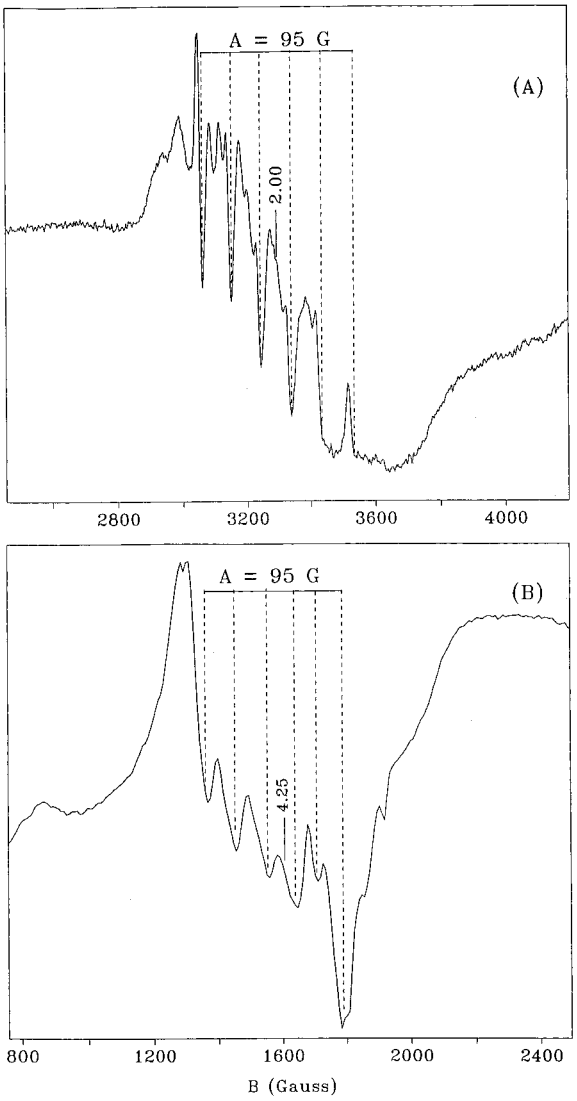

FIGURE 2: Expanded-scale EPR spectra of (A) 0.260 mM purified MndD as isolated, $g = 2$ region, and (B) 0.250 mM MndD + 2.7 mM 3,4-DHPA, anaerobic, $g = 4.25$ region. Temperature, 2.5 K; power, 0.02 mW at 9.23 GHz; modulation amplitude, 2 G.

approximately 95 G. This value is consistent with a Mn(II) coordinated octahedrally with oxygen or nitrogen ligands; lower values of A (60−70 G) are found for tetrahedral complexes or those with sulfur ligands (Reed & Markham, 1984). A five-coordinate geometry for MndD is possible as the trigonal bipyramidal Mn(II) center of manganese superoxide dismutase exhibits an A value of 85 G (Whittaker & Whittaker, 1991).

The forbidden hyperfine transitions and the shoulder-like features at $g = 1.6$ and 2.6 are due to the zero-field interactions. We have attempted to simulate these features using a combination of our own program and one from the literature (Reed & Markham, 1984). A match to the spectra has not yet been obtained; however, in order for the simulations to be close we find 150 G < D < 350 G, and E/D < 0.05. A survey of five other Mn(II)-containing proteins shows that their D values range from 250 to 350 G (Reed & Markham, 1984). Additional weak features are observed at $g = 4.3$ and 7.6, which are probably from a contaminating Fe(III) species.

The EPR spectrum of MndD is unchanged when the sample is rendered anaerobic, but changes significantly when

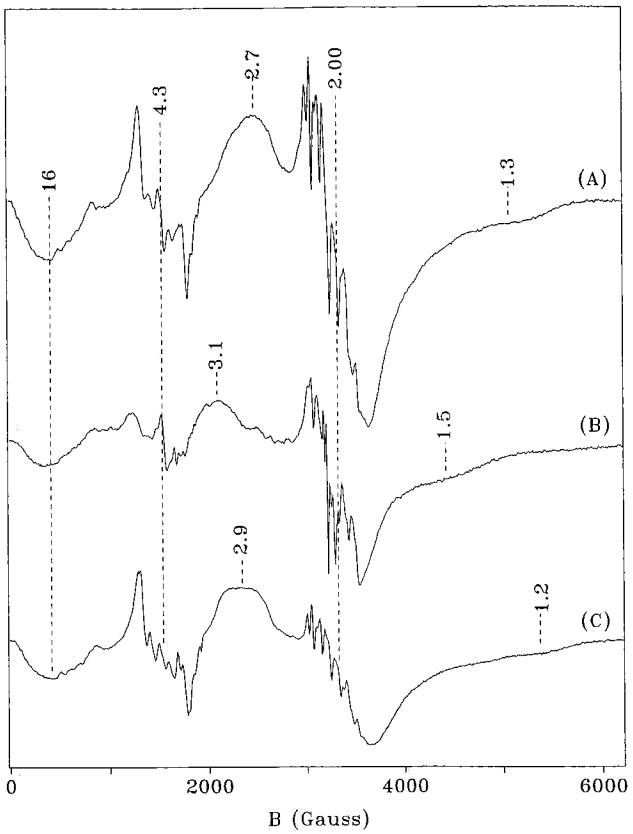

FIGURE 3: EPR spectra of (A) 0.165 mM MndD + 10.5 mM D,L-3,4-dihydroxymandelic acid, anaerobic; (B) 0.153 mM MndD + 8.5 mM *p*-nitrocatechol; and (C) 0.250 mM MndD + 2.7 mM 3,4-DHPA, anaerobic. Temperature, 2.5 K; power, 0.02 mW at 9.23 GHz; modulation amplitude, 10 G. All spectra are normalized to correct for differences in enzyme concentration and instrumental gain.

the substrate 3,4-DHPA is added under anaerobic conditions (Figure 3C). The intense signal at $g = 2$ with Mn hyperfine splitting is reduced significantly in intensity, and new features at $g = 1.2$, 2.9, 4.3, and 16 are observed. The $g = 4.3$ signal displays 6-fold hyperfine splitting ($A = 95$ G) that unambiguously assigns it to a Mn(II) center (see Figure 2B). In order to confirm that these EPR spectral changes do not correspond to irreversible alterations of the active site, the anaerobic MndD-3,4-DHPA samples were exposed to air, allowed to turn over, and then washed of product by a 3-fold dilution and reconcentration in a Centricon-30. The EPR spectrum of the resulting substrate-free sample is identical to that of the native enzyme as isolated (as in Figure 1A), demonstrating that the spectral changes that occur upon substrate binding are reversible.

Similar EPR changes are obtained with the addition of the good substrate D,L-3,4-dihydroxymandelate (Figure 3A) or the tight-binding inhibitor, *p*-nitrocatechol (Figure 3B). In contrast, the EPR spectra of the MndD complexes with the various weaker binding substrates and inhibitors (K_i = 0.5−7 mM) (Figures 1B−1D) show little or no difference from that of MndD as isolated. Although substrate-induced conformational changes cannot be ruled out, clearly there is a strong empirical correlation between molecules which exhibit strong binding at the active site (as demonstrated by low K_m or K_i) and the appearance of the intense $g = 4.3$ signal with ^{55}Mn hyperfine splitting.

EPR signals near $g = 4.3$ with 6-fold hyperfine structure have been observed for the Mn(II)-containing proteins

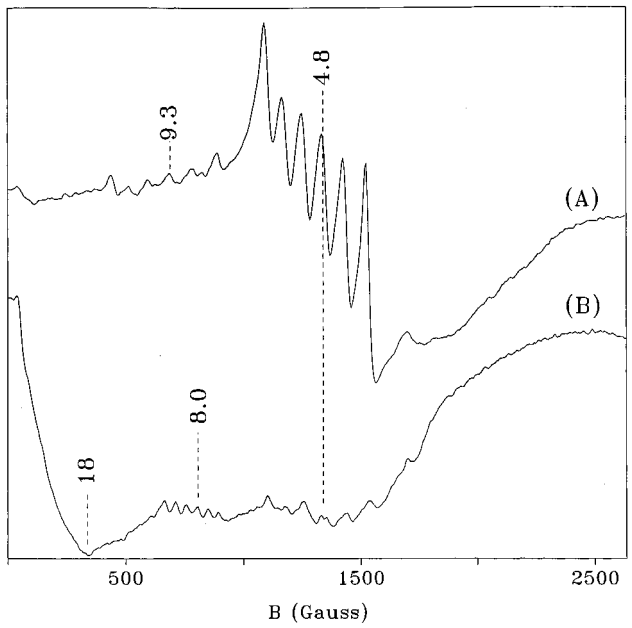

FIGURE 4: Parallel-mode EPR spectra of (A) 0.291 mM purified MndD as isolated, and (B) 0.250 mM MndD + 2.7 mM 3,4-DHPA, anaerobic. Temperature, 2.5 K; power, 0.20 mW at 9.08 GHz; modulation amplitude, 10 G.

phosphoglucomutase (Reed & Ray, 1971) and pyruvate kinase (Ash, 1982; Reed & Morgan, 1974) upon complexation with various strong binding substrates and inhibitors. In these cases the appearance of these lower-field signals has been attributed to large (5−10-fold) increases in ZFS caused by direct ligand coordination to the Mn(II) center (Reed & Markham, 1984). A simple physical model is that the substrate binding creates an electronic asymmetry about the Mn(II) center, especially when the new ligands are substantially weaker or stronger binding than those already present; this asymmetry results in increases in the parameters *D* and *E*. Our simulations of the MndD spectra show that a 2-fold increase in the ZFS will significantly increase the intensity of the "$\Delta M_s = \pm 2$" transition at $g = 4.3$ and create sizable anisotropy in the central fine-structure transition ($+1/2 \rightarrow -1/2$), rendering its hyperfine structure unresolvable. A better determination of the ZFS will require simulations of the spectra and a full assignment of all transitions.

Figure 4 shows EPR spectra acquired in parallel mode, where the probing microwave magnetic field ($\mathbf{B}_1$) is rotated from the standard configuration perpendicular to the main magnetic field ($\mathbf{B}$) to a parallel orientation. MndD as isolated (Figure 4A) displays a 6-fold hyperfine pattern at $g = 4.8$ and 9.3 ($A = 95$ G). These transitions have virtually no intensity for $\mathbf{B}_1 \perp \mathbf{B}$ but a modest amount for $\mathbf{B}_1 \parallel \mathbf{B}$. In the presence of substrate (Figure 4B) a hyperfine split signal is observed instead at $g = 8$ ($A = 50$ G). These spectra represent the first parallel-mode spectra observed for a biological Mn(II) center. While these signals have yet to be assigned, their existence suggests that parallel-mode EPR, which can be very useful for probing integer spin systems (Hendrich & Debrunner, 1989), may find further possible application to the study of these half-integer spin systems with relatively weak zero-field splitting.

DISCUSSION

We have purified an Mn-dependent 3,4-DHPA 2,3-dioxygenase, MndD, from *Arthrobacter globiformis* strain

Table 5: Survey of Known 3,4-DHPA 2,3-Dioxygenases

	Arthrobacter globiformis CM-2[a]	*Arthrobacter* Mn-1[b]	*Bacillus brevis*[c]	*Pseudomonas ovalis*[d]	*Klebsiella pneumoniae*[e]	*Bacillus stearothermophilus*[f]
molecular mass (Da)	155 444	172 000	140 000	140 000	102 000	106 000
subunit structure	4 × 38 861	4 × 43 000	4 × 36 000	4 × 35 000	4 × 25 500	3 × 35 000
metal content						
Mn^{2+}	2.8−3.3	1.1−2.1	1.9−2.1	nd[g]	0.01−0.3	nd
Fe^{2+}	0.4−1.0	0.2−1.9	0.04−0.20	4	<0.01	nd
Mg^{2+}	0	nd	nd	nd	1−1.3	nd
specific activity	9	10	6	30	102	0.275
pH optimum	7.0−8.2	8.0	7.5−8.0	nd	7.5	8.4−8.7
Fe^{2+} activation?	no	no	no	yes	no	no
H_2O_2 inactivation?	no	no	no	yes	yes	no

[a] This work. [b] Qi (1991). [c] Que et al. (1981). [d] Ono-Kamimoto (1973). [e] Gibello et al. (1994). [f] Jamaluddin (1977). [g] Not determined.

CM-2 to electrophoretic homogeneity via a four-step protocol that yields approximately 150 mg of protein from 100 g of cell mass. A batch extraction using 50% acetone greatly facilitates the purification of MndD and demonstrates its stability in organic solvent, a characteristic common to the extradiol-cleaving dioxygenases. The purified MndD consists of an α_4 homotetramer (4 × 38 861 Da) with an amino acid composition in close agreement with that predicted by the *mndD* gene sequence (Boldt et al., 1995).

MndD Specific Activity Correlates with Mn Content. A major goal of the initial characterization of MndD has been to determine its metal content and to determine to what extent it correlates with specific activity. The previously purified Mn-dependent enzymes from *B. brevis* (Que et al., 1981) and *Arthrobacter* Mn-1 (Qi, 1991) were both found to consist of homotetramers containing up to 2.1 g-atoms of Mn and varying amounts of Fe, whereas the Fe(II)-dependent enzymes from *P. ovalis* (Kita, 1965) and *Brevibacterium fuscum* (M. Miller, personal communication) were found to contain 4 g-atoms of Fe (see Table 5). This apparent half-occupation of the Mn-dependent enzymes could point to a possible structural difference in metal binding between the Fe- and Mn-dependent enzymes. However the results obtained here for MndD, using both ICP analysis and EPR spin quantitation, show it to contain 2.7−3.6 g-atoms of Mn (and 0.4−1.0 g-atoms of Fe) per homotetramer, indicating that 2 Mn per homotetramer is not an upper limit. Furthermore, it was found that the higher Mn content values were the direct result of using the extinction coefficient of the purified MndD rather than the Bradford method using a BSA standard which results in an erroneous protein concentration that is 50% higher. This discrepancy suggests that the values of 2 g-atoms of Mn per mole holoenzyme for the *B. brevis* and *Arthrobacter* Mn-1 enzymes, which were obtained using the Lowry and Bradford methods, respectively, might actually be closer to 3 g-atoms. It remains unclear why MndD (or either of the other two enzymes) is not fully occupied with 4 g-atoms of Mn; however, other dioxygenases have been found to have less than stoichiometric metal content. For example, protocatechuate 3,4-dioxygenase from *Pseudomonas putida* is composed of 12 identical subunits but typically contains only 7−8 g-atoms of Fe as isolated (Frazee, 1994).

The proposal that the 3,4-DHPA 2,3-dioxygenases from *B. brevis* and *Arthrobacter* Mn-1 require Mn was based initially on the oberved metal content of the purified enzymes and the inability of the bacteria to survive on 4-hydroxyphenylacetate as their sole carbon source without Mn in the growth medium. With the purification of larger quantities of MndD as described here, it has been possible to correlate directly its specific activity with Mn content. MndD as isolated has 3.0 ± 0.2 g-atoms of Mn and exhibits specific activities of 7.4−9.1 units/mg, while MndD partially or almost completely depleted of Mn shows proportionally lower specific activity (see "apo" and "partial-apo" entries in Table 4). Although some Fe (0.7 ± 0.2 g-atoms) has been found associated with MndD as isolated, its presence does not correlate strongly with specific activity. Further corroboration that Mn and not Fe is the active site metal center in MndD is derived from the dramatically different behaviors of MndD and the corresponding Fe-dependent enzyme from *P. ovalis* in the presence of potential inactivating reagents. The enzyme from *P. ovalis* is rapidly inactivated by H_2O_2 and $K_3Fe(CN)_6$, which oxidize the Fe(II) active site, and by CN^-, which probably extracts the Fe(II) (Ono-Kamimoto, 1973). In contrast, MndD is essentially unaffected by short-term exposure to these reagents. A similar contrast in reactivity has been noted for the Fe- and Mn-dependent superoxide dismutases (Asada et al., 1975; Lumsden et al., 1976). Moreover, whereas the addition of Fe(II) or ascorbate activates the *P. ovalis* enzyme, Fe(II) actually inactivates MndD and other members of this Mn-dependent subclass and ascorbate has no effect. The mechanism of Fe(II) inactivation is unclear, since $ZnCl_2$ (but not $MgCl_2$) also has the same effect. The proposal that Fe(II) or Zn(II) actually exchanges with Mn(II) in the active site to create an inactive enzyme is inconsistent with the result that the strong chelating reagent, 8-hydroxyquinolinesulfonate, at 1 mM concentration, does not inactivate MndD, suggesting a tightly bound Mn(II) ion. As Fe(II) and Zn(II) both cause rapid precipitation in the assay solutions (even in non-phosphate buffers at pH 7.5), it is more likely that they inactivate MndD through co-precipitation of the substrate, the product, and/or the enzyme itself.

The effect of H_2O_2 on 3,4-DHPA 2,3-dioxygenases deserves further comment. The Fe(II)-dependent enzyme from *P. ovalis* (Ono-Kamimoto, 1973) and the Mg(II)-dependent enzyme from *K. pneumoniae* (Gibello et al., 1994) are both rapidly and completely inactivated by H_2O_2, while MndD is not (see Table 5). Both the Fe(II)- and Mg(II)-dependent enzymes have significantly higher specific activities than MndD (∼9 units/mg) at 30 and 102 units/mg, respectively. Thus the higher oxidative resistance of MndD may come at the cost of lower specific activity. The 3,4-

DHPA 2,3-dioxygenase from *Bacillus stearothermophilus* (Jamaluddin, 1977) was also found to have a very low specific activity (in fact 21-fold lower than MndD) and high resistance to H_2O_2 inactivation, suggesting that it may also require Mn(II). Unfortunately, the specific metal content of this enzyme was not determined.

Substrate Likely Binds to the Metal Center of MndD. MndD catalyzes the extradiol cleavage of a variety of catechols but prefers substrates with a negatively charged carboxylate moiety. This preference is similar to that observed previously for other 3,4-DHPA 2,3-dioxygenases (Ono-Kamimoto, 1973; Que et al., 1981; Qi, 1991) and presumably arises from the presence of a carboxylate binding pocket in the enzyme active site. The lengthening of the substrate side chain by one methylene group is tolerated, but shortening the side chain by a methylene group is not. Indeed substrates lacking a carboxylate, catechol and 4-methylcatechol, are both turned over faster than 3,4-dihydroxybenzoate, suggesting that the latter, although having the necessary carboxylate moiety, lacks the appropriate interactions for efficient catalytic turnover.

The substrate hydroxyls are a significant binding determinant for MndD, as illustrated by the tight-binding of *p*-nitrocatechol, which is isosteric to 3,4-dihydroxybenzoate but inhibits with a 750-fold lower K_i. The distinctive feature of *p*-nitrocatechol is the *p*-nitro moiety, whose strongly electron-withdrawing nature significantly lowers the pK_a′s of the hydroxyl protons (p$K_{para} = 7$, p$K_{meta} = 11$) relative to unsubstituted catechol (p$K_1 = 9.8$, p$K_2 = 13$). Hence, the strong binding of *p*-nitrocatechol is most likely the result of its ability to undergo facile deprotonation of both of its hydroxyls to form a bidentate catecholate complex with the Mn center.

Support for this notion comes from analysis of the EPR spectra of MndD and its complexes with a variety of substrates and inhibitors. As isolated, MndD exhibits an EPR spectrum having an intense feature at $g = 2.0$ with well-resolved 6-fold hyperfine splitting of 95 G. Such a hyperfine splitting is typical of Mn(II) coordinated by non-sulfur ligand atoms in an octahedral (as opposed to tetrahedral) environment (Reed & Markham, 1984). Attempts to simulate the forbidden hyperfine transitions of the $g = 2.00$ signal as well as the shoulder-shaped signals at $g = 2.6$ and 1.6 lead to estimates of $D = 150-350$ G ($0.014-0.033$ cm^{-1}) and $E/D < 0.05$. This estimate of D overlaps the 250−350 G range that has been found in a wide variety of proteins in which Mn(II) is known to adopt an octahedral coordination geometry (Reed & Markham, 1984). Interestingly the MndD EPR spectrum is nearly indistinguishable from that of the *B. brevis* enzyme (Que et al., 1981). This level of identity extends to the distribution of line widths and intensities of the hyperfine lines (including the intensities of the forbidden hyperfine signals) across the whole $g = 2.00$ envelope, strongly suggesting that the Mn(II) centers of these two enzymes exist in identical coordination environments.

There is no change in the MndD spectrum under anaerobic conditions indicating that dioxygen does not bind directly to the Mn(II) center in the absence of substrate. The required prior binding of substrate for dioxygen binding is a common feature of the Fe(II)-dependent extradiol dioxygenases (Lipscomb & Orville, 1992) and appears to apply to the Mn(II) enzymes as well.

The binding of the substrate 3,4-DHPA to MndD under anaerobic conditions results in a dramatic change in the EPR spectrum of MndD with a decrease in the intensity of the $g = 2$ signal and the appearance of lower-field signals, particularly one at $g = 4.3$ with ^{55}Mn hyperfine splitting. Similar changes also occur with the complexes of the good substrate 3,4-dihydroxymandelic acid and the tight binding inhibitor *p*-nitrocatechol but not with any of the other substrates and inhibitors investigated. Though the precise basis for these changes is not well understood, it is clear that substrate binding is accompanied with a significant increase in the zero field splitting of the Mn(II) center. These spectral changes are very likely due to the coordination of substrate to the Mn(II) center.

Substrate binding to the Fe(II)-dependent dioxygenases appears to entail bidentate coordination to the metal center as suggested by MCD studies on the substrate complex of catechol 2,3-dioxygenase (Mabrouk et al.,1991) and EPR studies on the NO adduct of the protocatechuate 4,5-dioxygenase−substrate complex (Arciero et al., 1985). Preliminary analysis of BphC crystals in the presence of substrate supports this notion as the two bound solvent molecules of the five-coordinate active site appear to be displaced by the substrate hydroxyls (Sugiyama et al., 1995). Recent EXAFS studies on the substrate complex of catechol 2,3-dioxygenase suggest that only one hydroxyl proton is abstracted upon formation of the substrate complex (Shu et al., 1995). Moreover, it is proposed that this monoanionic substrate coordination is essential for extradiol cleavage, distinguishing it from the bidentate dianionic substrate found for the intradiol-cleaving enzymes (Orville & Lipscomb, 1989; True et al., 1990). It is not clear at present whether MndD also forms a similar monoanionic complex. However, the 14-fold lower K_i value for *m*-hydroxyphenylacetate relative to its *para* isomer does imply asymmetry in the manner the substrate binds to the metal center. This *meta* binding preference has also been observed for the corresponding Fe(II)-dependent enzyme from *B. fuscum* (M. Miller, personal communication), while a *para* binding preference is found for protocatechuate 4,5-dioxygenase, which catalyzes the cleavage of the C−C bond on the other side of the enediol unit relative to the side chain (Arciero et al., 1985). These observations hint at the importance of the metal−substrate interaction for steering the catalytic mechanism.

We have thus purified a Mn-dependent extradiol-cleaving catechol dioxygenase and characterized the Mn(II) center and its interactions with substrate and inhibitors. Considerable sequence homology exists between this enzyme and members of the family of Fe-dependent extradiol dioxygenases (Boldt et al., 1995). In light of the precedent set by the iron and manganese superoxide dismutase (Lah et al., 1995), it is reasonable to propose that the Mn(II) center of MndD may share the same coordination environment as the Fe(II) center in BphC. Recent site-directed mutagenesis studies of MndD support this proposal (Boldt, 1995). Future work will focus on further characterization of the enzyme active site and its mechanism of action.

ACKNOWLEDGMENT

We gratefully acknowledge Dr. Gerald Bratt (Department of Biochemistry, University of Minnesota), who carried out the sedimentation equilibrium experiment.

REFERENCES

Abragam, A., & Bleaney, B. (1970) *Electron Paramagnetic Resonance of Transition Ions*, Oxford University Press, London.

Arciero, D. M., Orville, A. M., & Lipscomb, J. D. (1985) *J. Biol. Chem. 260*, 14035−14044.

Asada, K., Yoshikawa, K., Takahashi, M., Maeda, Y., & Enmanji, K. (1975) *J. Biol. Chem. 250*, 2801−2807.

Ash, D. E. (1982) Ph.D. Thesis, University of Pennsylvania, Philadelphia, PA.

Bertini, I., Briganti, F., Mangani, S., Nolting, H. F., & Scozzafava, A. (1994) *Biochemistry 33*, 10777−10784.

Boldt, Y. R. (1995) Ph.D. Thesis, University of Minnesota.

Boldt, Y. R., Sadowsky, M. J., Ellis, L. B. M., Que, L., Jr., & Wackett, L. P. (1995) *J. Bacteriol. 177*, 1225−1232.

Bradford, M. (1976) *Anal. Biochem. 72*, 248−254.

Frazee, R. (1994) Ph.D. Thesis, University of Minnesota.

Gibello, A., Ferrer, E., Martin, M., & Garrido-Pertierra, A. (1994) *Biochem. J. 301*, 145−150.

Han, S., Eltis, L. D., Timmis, K. N., Muchmore, S. W., & Bolin, J. T. (1995) *Science 270*, 976−980.

Hendrich, M. P., & Debrunner, P. (1989) *Biophys. J. 56*, 489−506.

Jamaluddin, M. P. (1977) *J. Bacteriol. 129*, 690−697.

Kita, H. (1965) *J. Biochem. 58*, 116−122.

Laemmli, U. K. (1970) *Nature 227*, 680−685.

Lah, M. S., Dixon, M. M., Pattridge, K. A., Stallings, W. C., Fee, J. A., & Ludwig, M. L. (1995) *Biochemistry 34*, 1646−1660.

Lawrence, G. D., & Sawyer, D. T. (1978) *Coord. Chem. Rev. 27*, 173−193.

Lipscomb, J. D., & Orville, A. M. (1992) in *Metal Ions in Biological Systems* (Sigel, H., & Sigel, A., Eds.) Vol 28, pp 243−298, Marcel Dekker, Inc., New York.

Lipscomb, J. D., Whittaker, J. W., & Arciero, D. M. (1982) in *Oxygenases and Oxygen Metabolism* (Nozaki, M., Yamamoto, S., Ishimura, Y., Coon, M., Ernster, L., & Estabrook, R., Eds.) pp 27−38, Academic Press, New York.

Lowry, O. H., Rosebrough, N. J., Farr, A. L., & Randall, R. J. (1951) *J. Biol. Chem. 193*, 265−275.

Lumsden, J., Cammack, R., & Hall, D. O. (1976) *Biochim. Biophys. Acta 438*, 380−392.

Mabrouk, P. A., Orville, A. M., Lipscomb, J. D., & Solomon, E. I. (1991) *J. Am. Chem. Soc. 113*, 4053−4061.

Marquardt, D. W. (1963) *J. Soc. Ind. Appl. Math. 11*, 431.

Olson, P. E., Qi, B., Que, L., Jr., & Wackett, L. P. (1992) *Appl. Environ. Microbiol. 58*, 2820−2826.

Ono-Kamimoto, M. (1973) *J. Biochem. 74*, 1049−1059.

Orville, A. M., & Lipscomb, J. D. (1989) *J. Biol. Chem. 264*, 8791−8801.

Palmer, G. (1967) *Methods Enzymol. 10*, 595−609.

Qi, B. (1991) Masters Thesis, University of Minnesota.

Que, L. Jr. (1989) in *Iron Carriers and Iron Proteins* (Loehr, T. M., Ed.) pp 467−524, VCH, New York.

Que, L., Jr., Widom, J., & Crawford, R. L. (1981) *J. Biol. Chem. 256*, 10941−10944.

Reed, G. H., & Ray, W. J., Jr. (1971) *Biochemistry 10*, 3190−3197.

Reed, G. H., & Morgan, S. D. (1974) *Biochemistry 13*, 3537−3541.

Reed, G. H., & Markham, G. D. (1984) *Biol. Magn. Reson. 6*, 73−142.

Schachman, H. K. (1957) *Methods Enzymol. 4*, 32−104.

Shu, L., Chiou, Y.-M., Orville, A. M., Miller, M. A., Lipscomb, J. D., & Que, L., Jr. (1995) *Biochemistry 34*, 6649−6659.

Sugiyama, K. Senda, T., Narita, H., Yamamoto, T., Kimbara, K., Fukuda, M., Yano, K., & Mitsui, Y. (1995) *Proc. Jpn. Acad. 71B*, 32−35.

True, A. E., Orville, A. M., Pearce, L. L., Lipscomb, J. D., & Que, L., Jr. (1990) *Biochemistry 29*, 10847−10854.

Whittaker, J. W., & Whittaker, M. M. (1991) *J. Am. Chem. Soc. 113*, 5528−5540.

BI951979H